Strojniški vestnik - Journal of Mechanical Engineering 65(2019)1, 41-49
© 2019 Journal of Mechanical Engineering. All rights reserved.
DOI:10.5545/sv-jme.2018.5301
Original Scientific Paper
Received for review: 2018-02-20
Received revised form: 2018-07-07
Accepted for publication: 2018-08-09

Experimental Investigation of Newtonian and Non-Newtonian Liquid Flow in Wavy and Straight Mini-Channel Cross-Flow Plate Heat Exchangers

Ali Reza Anvari[1] – Koroush Javaherdeh[2,*]
[1] University of Guilan, Department of Mechanical Engineering, Iran
[2] University of Guilan, Faculty of Mechanical Engineering, Iran

In this research, an experimental study was performed regarding the heat transfer performance and pressure drop specifications of a Newtonian fluid and a non-Newtonian fluid. To this end, laminar flow of the deionized (DI) water and the aqueous solution containing 0.2 wt.% carboxyl methyl cellulose (CMC) were used as the Newtonian fluid and the non-Newtonian fluid, respectively, in wavy and straight mini-channel cross-flow heat exchangers (CFHE). Each mini-channel cross-flow plate heat exchanger (MCFPHE) was made of three copper plates for the hot and cold sides, which contain 27 mini-channels in parallel. The mini-channel CFHE was examined for Reynolds numbers (Re) in the range of 200 to 1800 and the hot-side inlet temperature was between 40 °C and 50 °C while the cold-side temperature varied in the range of 10 °C to 20 °C. The thermal and rheological properties of the non-Newtonian fluid were investigated. The results showed that for both fluids, the thermal performance of the wavy mini-channel is more than that of the straight mini-channel and, although the pressure drop was intensified, its effect is low at high Re values
Keywords: heat exchanger, mini-channel, non-Newtonian, CMC, wavy

Highlights
- *Non-Newtonian flow and convective heat transfer characteristics through straight and wavy micro-channels are experimentally investigated.*
- *Thermal and hydrodynamic performances of wavy micro-channels are investigated for different relative waviness.*
- *Results showed that the thermal and hydrodynamic performances increase with an increase in the relative waviness of wavy micro-channels.*

0 INTRODUCTION

The increasing industrial development of recent decades is directly linked to the improvement and development of new technologies. Heat exchangers are devices that are used to perform the thermal exchange between two fluids at different temperatures and, considering their wide applications, they have become the object of several research studies and developments. However, even along with this increasing evolution, the improvement of this system continues to be sought [1] and [2], aiming at both the conservation of energy and the elaboration of projects applied to specific situations. Among the several existing types, one of the best known is the plate heat exchanger. This type of equipment is widely used in various industrial segments and with numerous applications. Due to the need for smaller equipment with high effectiveness, micro- and mini-channel heat exchangers were developed. The higher volumetric heat transfer densities require advanced manufacturing techniques and more complex manifold designs. Dixit and Ghosh [3] summarized the manufacturing processes used in the fabrication of mini/micro-channel heat sinks and compared the different techniques related to tolerances and material compatibility. Naqiuddin et al. [4] reviewed the different geometric designs of mini/micro-channels, which were derived from numerical simulation and experimental works. Sidik et al. [5] comprehensively discussed the passive techniques for heat transfer augmentation in mini/micro-channels. Even though mini- and micro-channels can enhance the heat transfer rates significantly, it is not sufficient for some applications that need large heat fluxes. Thus, the usage of wavy channels has been considered. It was reported that wavy channels with larger wave amplitudes and shorter wavelengths [6], and channels employing coolants with nano-particles displayed better cooling performance. In another study, by Rostami et al. [7], water-Cu and water-Al_2O_3 as nanofluid was investigated in terms of heat transfer capability and fluid flow by using a rectangular micro-channel. It was shown that the Nusselt number increases with the increase in volume fraction and the decrease in particle diameter and that it is about three times higher for a nanofluid in a wavy micro-channel as compared to water in a straight micro-channel.

*Corr. Author's Address: Department of mechanical engineering, University of Guilan, Rasht, Iran, javaherdeh@guilan.ac.ir

The fluid flow and heat transfer capability of the TiO_2 nanofluid were studied by Arshad and Ali [8] experimentally in the straight mini-channel heat sink for laminar and transitional flows. The nanofluid containing 15 wt.% nanoparticle was used as a coolant. It is reported that the thermal performance of the nanofluid is a function of heating power, which could be enhanced at lower heating power. However, by decreasing the heating power, the pressure drop was increased.

Furthermore, Sohel et al. [9] have shown that the by using the nanofluid as a coolant, cooling performance is enhanced considerably. They have revealed that the nanoparticles in addition to enhancing the heat transfer, do not lead to excessive pressure. Thermal performance of a microprocessor was investigated by using pure water and nanofluid of Al_2O_3 and Cu by Siddiqui et al. [10]. It was observed that the Al_2O_3-water nanofluid yields significant performance in enhancing the heat transfer coefficient and reducing the thermal resistance. Also, by increasing the Reynolds number, the Cu-water nanofluid provided better results for thermal enhancement. Singh et al. [11] numerically confirmed the enhancement of the heat transfer in a 3D MHS by Nanofluids. The Nanofluids were found to increase the heat transfer rate compared to water. Parametric studies are carried out for different particle concentrations of 1, 3, and 5 vol.%. The particle size effect is observed for different particle sizes of 50 nm and 150 nm. In addition to the Nanofluid, non-Newtonian fluid [12] to [18] is an alternative for working fluid. Compared with Nanofluids, non-Newtonian fluids widely exist and can easily be prepared. Many common fluids such as solutions of polymers or surfactants, shows non-Newtonian fluid behaviour. The behaviour of non-Newtonian fluids is of great interest to many applications, including collecting, distributing, detecting, mixing and separating different types of biological and chemical species in a microchip. As a working fluid of a heat exchanger, for example, the heat transfer performance of non-Newtonian fluids was studied by Shamsi et al. [19] and Li et al. [20] in square micro-channels with triangular ribs and in a manifold micro-channel heat sink, respectively. They have reported that by increasing the volume fraction of the nanoparticles, the heat transfer is adversely affected.

Moreover, Li et al. [21] reported an increase in heat and mass transfer by non-Newtonian flows and noticed that the change in the dynamic viscosity of the materials in working chemical materials is the main reason for strengthening the secondary flow in the dimpled/protruded passage with flow separation. Pimenta and Campos [22] proved that the Nusselt numbers (Nu) for the non-Newtonian fluid flows in a spiral coil were, on mean, somewhat higher than those for Newtonian fluids because the viscous element of the shear-thinning polymer shows a tendency to affect the mixing effect of the Dean vortices. In the current work, the non-Newtonian characteristic of aqueous solutions containing 2 wt.% carboxyl methyl cellulose (CMC) was assessed, and calculations were also performed regarding the rheological behaviour of the non-Newtonian fluid. Furthermore, for a new cross-flow heat exchanger, pressure drop and heat transfer performance were studied with experiments with straight and wavy mini-channels.

1 MATERIALS AND METHODS

The CMC solutions were prepared by adding sodium carboxyl methyl cellulose with a nominal molecular weight of 900,000 [$gmol^{-1}$] and a DS of 0.8 to 0.95 (Dae-Jung company, South Korea) to distilled water, and agitating it on an electromagnetic stirrer at low axial speed for 2 h, to achieve complete hydration and avoiding the formation of air bubbles. The studied concentration was 0.2 *wt*.%. The specific heat c_p [Jkg^{-1} k^{-1}] and thermal conductivity k, were obtained for 0.2 % CMC solution, at temperatures between 40 °C and 50 °C. By adopting KD2 Pro (Decagon Devices, Inc., USA), the thermal conductivity and specific heat at constant were obtained for a non-Newtonian fluid. This is a portable device that is used in thermal analyses. For evaluating the specific heat (heat capacity) and thermal conductivity, the transient line heat source method is used with a KD2 device [23]. A small needle sensor (SH-1) was employed for assessing the specific heat in which the heat pulse method is used, and reliable values are obtained for specific heat capacity c_p by using nonlinear least square method during the processes. Only the SH-1 sensor can be considered for determining the specific heat, which is 30 mm in length and 1.28 mm in diameter and distance between two needles is 6 mm. By adopting this sensor, the thermal conductivity can also be determined [24] and [25]. The precision of this instrument is 5 % which meets the standards of EN 55022 [26] and IEEE 442-1987 [27]. The density of the CMC solution was determined in triplicates, by pycnometer. Rheological measurements were determined using a Rheometer (MCR 301 by Anton Paar, Graz, Austria) equipped with a cone-and-plate geometry (angle: 0.034 rad, diameter: 40 mm). The shear rate was varied between 12.2 s^{-1} and 200 s^{-1}, and both upward and downward tests were performed in duplicate for the CMC solution, at five different temperatures between 10 °C and 50 °C.

2 EMPIRICAL SETUP AND METHODOLOGY

An experimental setup has been developed to examine the heat transfer characteristics and the drop in the pressure of the wavy and straight mini-channels under different flow conditions as shown in Fig. 1. It consists of two parts: a hot fluid and a cold fluid. For maintaining the inlet temperature and flow velocity at constant values, a thermostatic bath, a controllable magnetic gear pump and a paddle wheel flow meter were used for each part of the setup. Two filters were installed at the entrance of each flow meter to remove the external matter in the liquid and to prevent fluctuations and the rusting of the flow meter. Insulation is applied throughout the unit in an experimental setting in order to minimize the heat loss. Thermocouples, as well as absolute and differential pressure transmitters, were installed on all inputs and outputs. Before starting each experiment, each measuring device was calibrated. Non-Newtonian fluid flow rate has been varied in a range of 0.5 Lmin^{-1} to 4 Lmin^{-1} whereas the inlet hot stream temperature ranges from 40 °C to 50 °C. The cold stream flow rate has been varied in range of 0.5 Lmin^{-1} to 4 Lmin^{-1} along with inlet temperature being in a range of 10 °C to 20 °C. A typical test usually takes about 20 minutes. A time interval was needed for the system to achieve stable conditions. To verify that such conditions have reached a stable state, the temperature was monitored continuously. Once the thermal equilibrium conditions were obtained, the flow rate and temperature readings were recorded. The average values of the measurements were recorded beside the estimated errors.

The heat exchanger plate used in this study was fabricated from copper alloy. Each plate was 80 mm in width and 80 mm in length, and the thickness is 2 mm. The wavy and straight mini-channels with cross-sectional dimensions of 1 mm in width and 1 mm depth were machined with a CNC machine. Schematic patterns of the constructed plates with two keyway dimensions are shown in Fig. 2.

As can be observed in the figure, specific geometrical parameters of wavy channels can be considered for investigating the relative waviness ($2A/2L$). In this regard, in the current research, the impact of such parameters on the performance of cross-flow heat exchangers was studied on two levels of relative waviness (i.w. $2A/2L$ = 0.2 and 0.3). The

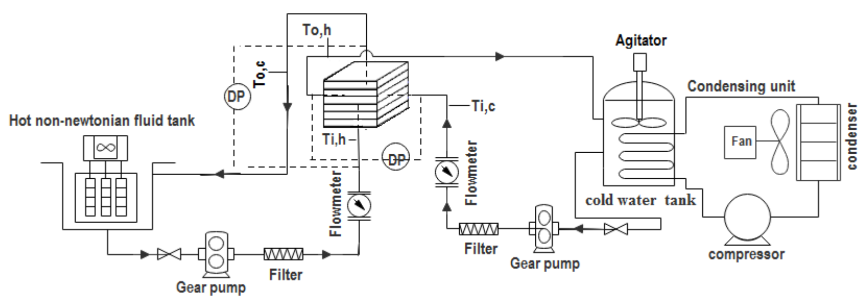

Fig. 1. *Schematic diagram of the experimental setup*

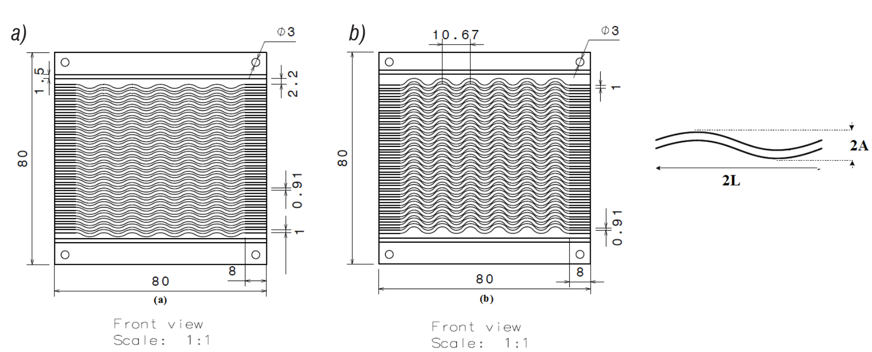

Fig. 2. *Schematic of a repeating unit of wavy mini-channels; a) 2A/2L=0.2, b) 2A/2L=0.3*

dimensions of the mini-cross-flow heat exchanger are also tabulated in Table 1.

Table 1. *Geometrical parameters of tested plate heat exchanger*

Parameter	Value
Wave amplitude [2A]	2.2, 3.2
Dimensions of heat exchanger (w×l×h)[mm]	100×100×22
Dimensions of plates (w×l×t) [mm]	80×80×2
Wavelength (2L) [mm]	10.67
Thermal conductivity of plate material [Wm^{-1}k^{-1}]	385
Total number of channels	27
Number of channels per plate	6

2.1 Thermal Physical Properties of CMC Aqueous Solutions

Specific heat capacity and thermal conductivity were determined at three different temperatures. Fig. 3 shows the viscosity against the shear stress of the CMC aqueous solution at different temperatures. By increasing the shear rate, the viscosity of the CMC aqueous solutions decreases, also at the same shear rate, the viscosity of the CMC aqueous solutions increases with decreases in temperature.

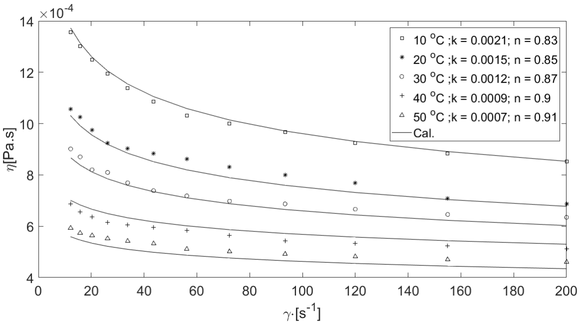

Fig. 3. *The relation of viscosity and shear rate for CMC aqueous solution*

It is disclosed that the CMC solutions present shear-thinning behaviour. However, the CMC aqueous solutions follow the power law model, given in Eq. (1), with a flow behaviour index or power law index of less than unity (n < 1) [28] and [29]:

$$\eta = K\gamma^{n-1}. \quad (1)$$

In Eq. (1) η [Pa·s] is the apparent viscosity, γ [s^{-1}] is the shear rate, and parameters K and n [m] are the consistency index and the power law index, respectively.

3 RESULTS AND DISCUSSION

Experiments were conducted for two wavy channels with different relative waviness (2A/2L) of the wavy mini-channels and in the presence of CMC to study the effects of these parameters on heat transfer capability and friction factor. Initial tests were also performed for a straight channel and base fluid to validate the experiment procedure and form baselines for the comparison. The inlet temperature for the hot liquid was 40 °C and 50 °C, with a cold water temperature of 10 °C to 20 °C. The hot and cold flow rate in Reynolds was measured from 200 to 600. The heat transfer rate in hot and cold fluids through the test section can be achieved using $\dot{Q} = \dot{m} c_p \Delta T$. By considering the logarithmic temperature average (LMTD), the heat transfer coefficient (U) can be evaluated:

$$\Delta T_{LMTD} = \frac{(T_{i,hot} - T_{o,cold}) - (T_{o,hot} - T_{i,cold})}{\ln\left\{(T_{i,hot} - T_{o,cold}) - (T_{o,hot} - T_{i,cold})\right\}}, \quad (2)$$

and mean heat transfer $\dot{Q}_m$ [W], via

$$U = \frac{\dot{Q}_m}{F\, A_S\, \Delta T_{LMTD}}. \quad (3)$$

That A_S [m^2] is the total heat transfer area and $\dot{Q}_m = \left(\dot{Q}_{hot} + \dot{Q}_{cold}\right)/2$. Also, the coefficient factor F for the cross-flow heat exchanger in this equation is 0.97. The hydraulic diameter is calculated using the proposed method by [30] as:

$$d_h = \frac{4V_S}{A_S}, \quad (4)$$

where V_S [m^3] is the enclosed (wetted) volume. For power law fluids, Tang et al. [32] introduced a new generalized Re. For power law fluid flow, the generalized Re for non-Newtonian fluid is presented as:

$$\mathrm{Re} = \frac{\rho\, d_h^n\, u^{2-n}}{k}\left(\frac{n}{a+bn}\right)^n 8^{1-n}, \quad (5)$$

where ρ [kgm^{-3}] and u [ms^{-1}] are density and the average velocity of the fluid respectively, and k and n are the rheological parameters that are obtained from Eq. (1), for the CMC solution. The constants are $a = 0.2121$ and $b = 0.6766$ for square cross-sectional channels [31]. It is noteworthy that the heat transfer coefficients of the hot and cold loop should be calculated independently.

The Fanning friction factor was also calculated using the following equation:

$$f = \frac{1}{2}\frac{d_h\, \Delta P / L}{\rho\, u^2}. \quad (6)$$

In plate heat exchanger (PHE) experiments, the temperatures, flow rates and pressure loss were measured by employing appropriate instruments.

During the measurements, uncertainties of the PHE results were estimated by Moffat's theory [32]. In this theory, Moffat has defined the final result (Y) as a function of different measured variables, X_i, through $Y=f(X_1,X_2,\ldots,X_n)$. According to this theory, the contribution of the uncertainty to each variable can be estimated by:

$$\frac{U_Y}{Y}=\frac{\sqrt{\left(\frac{\partial Y}{\partial X_1}U_{X_1}\right)^2+\ldots+\left(\frac{\partial Y}{\partial X_n}U_{X_n}\right)^2}}{f\left(X_1,X_2,\ldots,X_n\right)}. \quad (7)$$

The overall uncertainty for the estimated results is given in Table 2. Repeated tests show that all the sets of the experimental data are within the uncertainty limits.

Table 2. *Parameters and estimated uncertainty*

Instrument / parameters	Model	Accuracy
Flow meter [l/min]	Fotek - KTM	±0.5 % of readings**
Thermocouples [T]	Type-T	±1.0 [°C] of readings**
Pressure transmitter [p]	EWDT-2.5	≤1%**
Pump [24DC]	Gear pump	Head 21 meter
PID controller	Delta	±1% of readings*
Bolt heater [W]	2000	±2% of readings**
Thermo-physical properties		
Viscosity	Brookfield	±2.5% of readings*
Density	Anton paar, MCR 301	±3% of readings*
Thermal conductivity	Decagon KD2-Pro	±5% of readings*
Specific heat	Decagon KD2-Pro	±5% of readings*
Calculated parameters		
Reynolds number of hot and cold side	Moffat	±1% to 2%
Heat transfer coefficient of hot and side	Moffat	±6% to 7%
Friction factor	Moffat	±6%

* Based on manufacturer claim
**Based on the calibration process

3.1 Validation

To validate the present experimental results and form a baseline for comparison, the initial tests are conducted for the water flow in the straight mini-channel cross-flow heat exchanger. The straight mini-channel has the same number of mini-channels and magnitude of geometrical parameters as the wavy channel. The fitted curve of the heat transfer rate is calculated using correlations of Nu proposed by Shah and London and Stephan and Preuβer [33] and [34] which are used to validate the experimental data of heat transfer rate as depicted in Fig. 4 for the water flow against the Re of the cold fluid. As shown in the figure, the obtained results in the present study are in good agreement with analytical analysis. For estimating the heat transfer coefficient, the following relation is employed:

$$U=\frac{1}{\frac{1}{h_{hot}}+\frac{1}{h_{cold}}+\frac{t}{K_{cooper}}}, \quad (8)$$

where t [mm] is the thickness of the plate, K_{cooper} [$Wm^{-1}k^{-1}$] is the thermal conductivity of copper (the heat exchanger has been fabricated from copper), h_{hot} [$Wm^{-2}k^{-1}$] and h_{cold} [$Wm^{-2}k^{-1}$] are the convective heat transfer coefficients of the hot and cold water, respectively. The correlations overestimate the obtained results. However, it can be related to the fouling resistances that are ignored during the calculations and, considering the fact that the correlations are empirical, the obtained data would be acceptable.

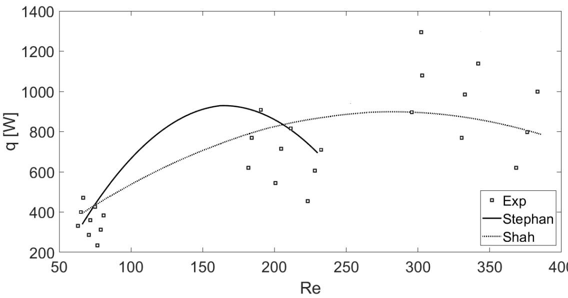

Fig. 4. *Experimental evaluation compared to calculated using correlations by Shah and London and Stephan and Preuβer*

3.2 Effect of Geometrical Parameters

There are three submissive mechanisms [35] that enhance the heat transfer rate in single-phase flow, including: (1) decrease in thickness of the thermal boundary layer, (2) increase in fluid disturbance [36] and [37]; and (3) increase in gradient velocity in vicinity of the heat transfer wall. When the fluid flows in wavy channels, disturbance of the streamlines of the flow occurs [38] to [40]. Mixing of the flow is the result of this interruption and, as a consequence, the heat transfer capability is enhanced. The regions that possess the maximum amplitude values in a wavy channel initiate the vortices and secondary flows.

While flowing the liquid through curved passages, the liquid is exposed to centrifugal force resulting in secondary flow, which is commonly known as Dean Vortices or chaotic advection; as vortices are formed, the fluid undergoes a rapid shearing and stretching, which results in better fluid mixing and, consequently, higher rates of heat transfer are acquired.

In addition, the pressure near the outer concave wall is increased due to the centrifugal force in the curvature of the channel and, as a result, the pressure gradient is enhanced toward the centre of the flow. Considering this pressure gradient, the high-pressure fluid is moved from the outer region toward the core [41].

However, all these processes enhance not only the heat transfer rate but also the pressure drop. Fig. 5a shows the variations of *q* as a function of Re. It is clear that the higher heat transfer is obtained for a wavy mini-channel cross-flow heat exchanger (MCFPHE) compared with the straight channels in which the heat transfer rate is increased with the relative waviness. The analysis of *U* vs. Re of the cold fluid confirms this conclusion as shown in Fig. 5b.

3.3 Effect of Non-Newtonian Behaviour

The viscosity increase caused by the CMC dissolution in water can affect the flow pattern or flow regime considerably. To study the effects of the non-Newtonian fluid, i.e. the water–CMC mixtures, the variations of the q as a function of the Re are shown in Fig. 6. According to this figure, the same conclusion regarding the wavy effect of Newtonian fluid can be drawn. However, higher heat transfer values compared to the Newtonian fluid are obtained at all configurations.

3.4 Pressure Drop Characteristics

Experiments showed that using the CMC/water non-Newtonian fluids can slightly enhance the pressure drop in comparison to the base fluid. In fact, the presence of CMC inside the water can enhance the viscosity and, as a result, higher values of pressure drop are obtained for the non-Newtonian fluids.

Fig. 7 compares the pressure drop of the systems with water and CMC solution as hot fluid versus Re of the hot fluid. According to this figure, the ratio is always higher than 1, which verifies the above-mentioned conclusion in comparing the non-Newtonian and Newtonian fluids. The effect of temperature is negligible and wavy 2 (with higher relative waviness) shows the least pressure drop ratio, especially at higher Re.

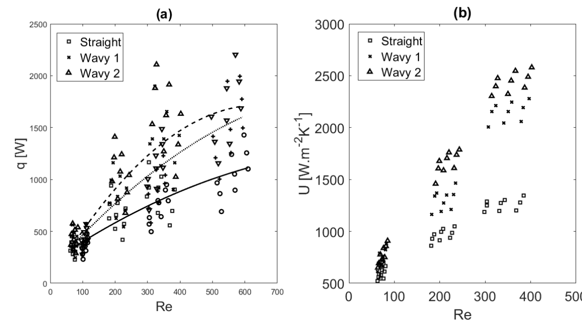

Fig. 5. *Experimental data for a) heat transfer, q and b) heat transfer coefficient of MCFPHE using water as hot and cold fluid*

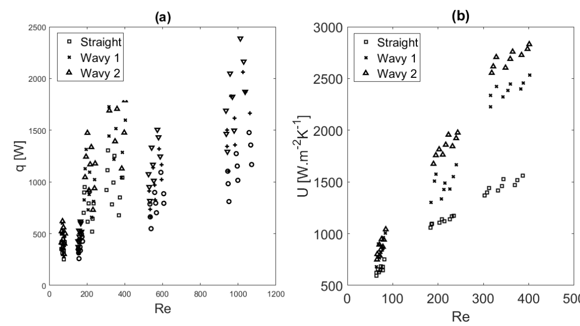

Fig. 6. *Experimental data for a) heat transfer, q and b) heat transfer coefficient, U of MCFPHE using water as cold fluid and CMC solution as hot fluid*

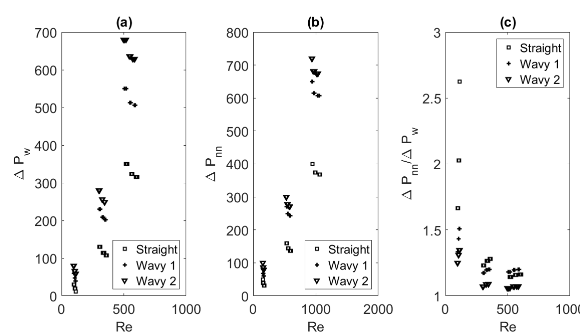

Fig. 7. *The pressure drop of MCFPHE with water as cold fluid and a) water as hot fluid, b) CMC solution as hot fluid, and c) the ratio of CMC and water pressure drop*

The experimental results of the friction factor are shown in Fig. 8. According to Fig. 8a for water and Fig. 8b for CMC, the friction factor of the wavy channel is always higher than that of the straight channel; however, according to Fig. 8c the influence of non-Newtonian fluid in enhancing the pressure drop is less in the case of wavy MCFPHE with higher relative waviness.

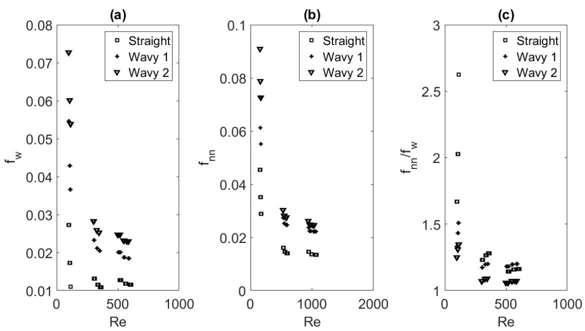

Fig. 8. *Friction factor of MCFPHE with water as cold fluid and a) water as hot fluid, b) CMC solution as hot fluid, and c) the ratio of CMC and water friction factor*

3.5 Overall Performance Factor (PF)

To investigate the performance of wavy passages, the heat transfer performance of the two wavy channel configurations is compared along with the pressure drop. Fig. 9 shows the performance evaluation criterion (PEC) as a function of the Reynolds number. It was calculated from Eq. (9) **[42]**.

$$PEC = \frac{U_{nn}/U_{ws}}{\left(f_{nn}/f_{ws}\right)^{0.333}}, \qquad (9)$$

where U_n and f_n are heat transfer coefficient and friction factors of a non-Newtonian fluid flow in a wavy and straight channel with different relative waviness and the U_{ws} and f_{ws} are heat transfer coefficient and friction factors of a DI water in a straight, respectively. It is clear that when the PEC is higher than unity, the applied technique is more in favour of heat transfer improvement rather than increasing the pressure drop.

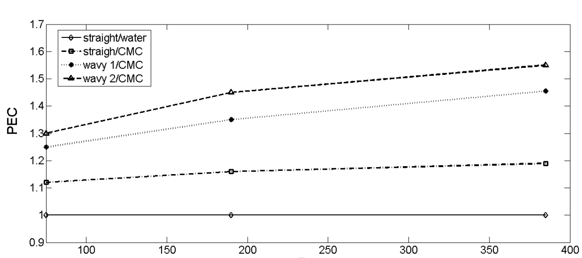

Fig. 9. *Performance evaluation criterion versus Reynolds number for various working fluids in MCFPHE*

The geometric parameters, the working fluid composition, and the Reynolds number affect the amount of this parameter. From Fig. 9, it is clear that for each case, the PEC increases approximately as the Reynolds increases, and the overall improvement due to the wave channel in the higher flow current is significant. Also, for a given flow rate, the non-Newtonian fluid with higher weight fraction has higher values of the PEC.

4 CONCLUSION

In this research work, the thermal-hydraulic performance of a wavy mini-channel cross-flow heat exchanger was studied using the CMC/water as non-Newtonian fluid, and the effects of relative waviness (A/L), non-Newtonian fluid, and Reynolds number were studied. The results obtained for the straight MCHS were first confirmed by considering the previous works for which a reasonable agreement was established. It was observed that for all considered cases, higher heat transfer was obtained for the wavy channel compared with a straight channel. The CMC/water non-Newtonian showed better heating performance compared with the base fluid. The pressure drop of the wavy mini-channels was higher than that of the straight mini-channels. This is due to the change of the geometrical parameter, especially with relative waviness (A/L) change. It is suggested that applying the combined method (i.e. simultaneous use of wavy mini-channels and non-Newtonian fluid) as proposed in this research, can be a good choice in practical applications to enhance the heat transfer performance of cross-flow mini-channel heat exchangers.

5 REFERENCES

[1] Hussein, N.F. (2018). Experimental investigation of using new shape augmentations for enhancing heat transfer in heat exchanger. *Journal of Engineering and Sustainable Development*, vol. 21, no. 6, p. 80-91.

[2] Balaji, K., Iniyan, S., Muthusamyswami, V. (2017). Experimental investigation on heat transfer and pumping power of forced circulation flat plate solar collector using heat transfer enhancer in absorber tube. *Applied Thermal Engineering*, vol. 112, p. 237-247, **DOI:10.1016/j.applthermaleng.2016.09.074**.

[3] Dixit, T. Ghosh, I. (2015) Review of micro-and mini-channel heat sinks and heat exchangers for single phase fluids. *Renewable and Sustainable Energy Reviews*, vol. 41, p. 1298-1311, **DOI:10.1016/j.rser.2014.09.024**.

[4] Naqiuddin, N.H., Saw, L.H., Yew, M.C., Yusof, F., Ng. T.C., Yew, M.K. (2018). Overview of micro-channel design for high heat flux application. *Renewable and Sustainable Energy Reviews*, vol. 82, p. 901-914, **DOI:10.1016/j.rser.2017.09.110**.

[5] Sidik, N.A.C., Muhamad, M.N.A.W., Japar, W.M.A.A., Rasid, Z.A. (2017). An overview of passive techniques for heat transfer augmentation in microchannel heat sink. *International Communications in Heat and Mass Transfer*, vol. 88, p. 74-83, **DOI:10.1016/j.icheatmasstransfer.2017.08.009**.

[6] Lin, L., Zhao, J., Lu, G., Wang, X.-D., Yan, W.-M. (2017). Heat transfer enhancement in microchannel heat sink by wavy channel with changing wavelength/amplitude. *International Journal of Thermal Sciences*, vol. 118, p. 423-434, DOI:10.1016/j.ijthermalsci.2017.05.013.

[7] Rostami, J., Abbassi, A., Harting, J. (2018). Heat transfer by nanofluids in wavy microchannels. *Advanced Powder Technology*, vol. 29, no. 4, p. 925-933, DOI:10.1016/j.apt.2018.01.010.

[8] Arshad, W., Ali, H.M. (2017). Experimental investigation of heat transfer and pressure drop in a straight minichannel heat sink using TiO_2 nanofluid. *International Journal of Heat and Mass Transfer*, vol. 110, p. 248-256, DOI:10.1016/j.ijheatmasstransfer.2017.03.032.

[9] Sohel, M.R., Khaleduzzaman, S.S., Saidur, R., Hepbasli, A., Sabri, M.F.M., Mahbubul, I.M. (2014). An experimental investigation of heat transfer enhancement of a minichannel heat sink using Al_2O_3–H_2O nanofluid. *International Journal of Heat and Mass Transfer*, vol. 74, p. 164-172, DOI:10.1016/j.ijheatmasstransfer.2014.03.010.

[10] Siddiqui, A.M., Arshad, W., Ali, H.M., Ali, M., Nasir, M.A. (2017). Evaluation of nanofluids performance for simulated microprocessor. *Thermal Science*, vol. 21, no. 5, p. 2227-2236, DOI:10.2298/TSCI150131159S.

[11] Singh, P.K., Naruka, D.S., Seng, L.P. (2018). Numerical investigation of flow and heat transfer of nanofluids in a wavy microchannel. *International Journal of Energy for a Clean Environment*, vol. 19, no. 1-2, p. 19-35, DOI:10.1615/InterJEnerCleanEnv.2018021099.

[12] Sajadifar, S.A., Karimipour, A., Toghraie, D. (2017). Fluid flow and heat transfer of non-Newtonian nanofluid in a microtube considering slip velocity and temperature jump boundary conditions. *European Journal of Mechanics-B/Fluids*, vol. 61, p. 25-32, DOI:10.1016/j.euromechflu.2016.09.014.

[13] Shojaeian, M., Koşar, A. (2016). Convective heat transfer of non-Newtonian power-law slip flows and plug flows with variable thermophysical properties in parallel-plate and circular microchannels. *International Journal of Thermal Sciences*, vol. 100, p. 155-168, DOI:10.1016/j.ijthermalsci.2015.09.024.

[14] Shojaeian, M., Yildiz, M., Koşar, A. (2015). Convective heat transfer and second law analysis of non-Newtonian fluid flows with variable thermophysical properties in circular channels. *International Communications in Heat and Mass Transfer*, vol. 60, p. 21-31, DOI:10.1016/j.icheatmasstransfer.2014.12.002.

[15] Stocks, M.D., Bello-Ochende, T., Meyer, J.P. (2014). Maximum thermal conductance for a micro-channel, utilising Newtonian and non-Newtonian fluid. *Heat and Mass Transfer*, vol. 50, no. 6, p. 865-875, DOI:10.1007/s00231-014-1298-0.

[16] Ellahi, R. (2013). The effects of MHD and temperature dependent viscosity on the flow of non-Newtonian nanofluid in a pipe: analytical solutions. *Applied Mathematical Modelling*, vol. 37, no. 3, p. 1451-1467, DOI:10.1016/j.apm.2012.04.004.

[17] Prasad, K.V., Vajravelu, K., Vaidya, H., Raju, B.T. (2015). Heat transfer in a non-Newtonian nanofluid film over a stretching surface. *Journal of Nanofluids*, vol. 4, no. 4, p. 536-547, DOI:10.1166/jon.2015.1174.

[18] Ternik, P., Rudolf, R., Žunič, Z. (2015). Heat-transfer characteristics of a non-Newtonian Au nanofluid in a cubical enclosure with differentially heated side walls. *Materials and Technology*, vol. 49, no. 1, p. 87-93.

[19] Shamsi, M.R., Akbari, O.A., Marzban, A., Toghraie, D., Mashayekhi, R. (2017). Increasing heat transfer of non-Newtonian nanofluid in rectangular microchannel with triangular ribs. *Physica E: Low-dimensional Systems and Nanostructures*, vol. 93, p. 167-178, DOI:10.1016/j.physe.2017.06.015.

[20] Li, S.-N., Zhang, H.-N., Li, X.-B., Li, Q., Li, F.-C., Qian, S., Joo, S.W. (2017). Numerical study on the heat transfer performance of non-Newtonian fluid flow in a manifold microchannel heat sink. *Applied Thermal Engineering*, vol. 115, p. 1213-1225, DOI:10.1016/j.applthermaleng.2016.10.047.

[21] Li, P., Zhang, D., Xie, Y., Xie, G. (2016). Flow structure and heat transfer of non-Newtonian fluids in microchannel heat sinks with dimples and protrusions. *Applied Thermal Engineering*, vol. 94, p. 50-58, DOI:10.1016/j.applthermaleng.2015.10.119.

[22] Pimenta, T.A., Campos, J.B.L.M. (2013). Heat transfer coefficients from Newtonian and non-Newtonian fluids flowing in laminar regime in a helical coil. *International Journal of Heat and Mass Transfer*, vol. 58, no. 1-2, p. 676-690, DOI:10.1016/j.ijheatmasstransfer.2012.10.078.

[23] Amrollahi, A., Rashidi, A.M., Lotfi, R., Meibodi, M. E., Kashefi, K. (2010). Convection heat transfer of functionalized MWNT in aqueous fluids in laminar and turbulent flow at the entrance region. *International Communications in Heat and Mass Transfer*, vol. 37, no. 6, p. 717-723, DOI:10.1016/j.icheatmasstransfer.2010.03.003.

[24] Sanuade, O.A., Adesina, R.B., Amosun, J.O., Fajana, A.O., Olaseeni, O.G. (2017). Using artificial neural network to predict dry density of soil from thermal conductivity. *Materials and Geoenvironment*, vol. 64, no. 3, p. 169-180, DOI:10.1515/rmzmag-2017-0012.

[25] Siddiqui, O.K., Zubair, S.M. (2017). Efficient energy utilization through proper design of microchannel heat exchanger manifolds: A comprehensive review. *Renewable and Sustainable Energy Reviews*, vol. 74, p. 969-1002, DOI:10.1016/j.rser.2017.01.074.

[26] EN 55022 (2010). *Information Technology Equipment - Radio Disturbance Characteristics - Limits and Methods of Measurement*, CENELEC, Brussels.

[27] IEEE 854 (1987). *The Standard for Radix-Independent Floating-Point Arithmetic*, Institute of Electrical and Electronics Engineers (IEEE), Piscataway.

[28] Abdelrahim, K.A., Ramaswamy, H.S. (1995). High temperature/pressure rheology of carboxymethyl cellulose (CMC). *Food Research International*, vol. 28, no. 3, p. 285-290, DOI:10.1016/0963-9969(94)00045-A.

[29] Yaşar, F., Toğrul, H., Arslan, N. (2007). Flow properties of cellulose and carboxymethyl cellulose from orange peel. *Journal of Food Engineering*, vol. 81, no. 1, p. 187-199, DOI:10.1016/j.jfoodeng.2006.10.022.

[30] Hesselgreaves, J.E., Law, R., Reay, D. (2016). *Compact Heat Exchangers: Selection, Design and Operation*. Butterworth-Heinemann, Oxford.

[31] Tang, G.H., Lu, Y.B., Zhang, S.X., Wang, F.F., Tao, W.Q. (2012). Experimental investigation of non-Newtonian liquid flow in microchannels. *Journal of Non-Newtonian Fluid Mechanics*, vol. 173-174, p. 21-29, DOI:10.1016/j.jnnfm.2012.02.001.

[32] Moffat, R.J. (1982). Contributions to the theory of single-sample uncertainty analysis. *Journal of Fluids Engineering*, vol. 104, no. 2, p. 250-258, **DOI:10.1115/1.3241818**.

[33] Stephan, K., Preußer, P. (1979). Wärmeübergang und maximale Wärmestromdichte beim Behältersieden binärer und ternärer Flüssigkeitsgemische. *Chemie Ingenieur Technik*, vol. 51, no. 1, p. 37-37, **DOI:10.1002/cite.33051112**. (in German)

[34] Mortean, M.V.V., Paiva, K.V., Mantelli, M.B.H. (2016). Diffusion bonded cross-flow compact heat exchangers: Theoretical predictions and experiments. *International Journal of Thermal Sciences*, vol. 110, p. 285-298, **DOI:10.1016/j.ijthermalsci.2016.07.010**.

[35] Tao, W.Q., He, Y.L., Wang, Q.W., Qu, Z.G., Song, F.Q. (2002). A unified analysis on enhancing single phase convective heat transfer with field synergy principle. *International Journal of Heat and Mass Transfer*, vol. 45, no. 24, p. 4871-4879, **DOI:10.1016/S0017-9310(02)00173-4**.

[36] Wang, Y., Ling, X. (2016). Experimental and numerical studies of fluid flow confined in microchannel. *ASME 5th International Conference on Micro/Nanoscale Heat and Mass Transfer*, p. no.MNHMT2016-6671, **DOI:10.1115/MNHMT2016-6671**.

[37] Chai, L., Wang, L. (2018). Thermal-hydraulic performance of interrupted microchannel heat sinks with different rib geometries in transverse microchambers. *International Journal of Thermal Sciences*, vol. 127, p. 201-212, **DOI:10.1016/j.ijthermalsci.2018.01.029**.

[38] Sui, Y., Teo, C.J., Lee, P.S. (2012). Direct numerical simulation of fluid flow and heat transfer in periodic wavy channels with rectangular cross-sections. *International Journal of Heat and Mass Transfer*, vol. 55, no. 1-3, p. 73-88, **DOI:10.1016/j.ijheatmasstransfer.2011.08.041**.

[39] Sui, Y., Teo, C.J., Lee, P.S., Chew, Y.T., Shu, C. (2010). Fluid flow and heat transfer in wavy microchannels. *International Journal of Heat and Mass Transfer*, vol. 53, no. 13-14, p. 2760-2772, **DOI:10.1016/j.ijheatmasstransfer.2010.02.022**.

[40] Sui, Y., Lee, P.S., Teo, C.J. (2011). An experimental study of flow friction and heat transfer in wavy microchannels with rectangular cross section. *International Journal of Thermal Sciences*, vol. 50, no. 12, p. 2473-2482, **DOI:10.1016/j.ijthermalsci.2011.06.017**.

[41] Yang, C S., Jeng, D.Z., Liu, C.W., Liu, C.G., Gau, C. (2010). Fluid flow and heat transfer in a horizontal channel with divergent top wall and heated from below. *Journal of Heat Transfer*, vol. 132, no. 8, p. 081403, **DOI:10.1115/1.4001606**.

[42] Karwa, R., Sharma, C., Karwa, N. (2013). Performance evaluation criterion at equal pumping power for enhanced performance heat transfer surfaces. *Journal of Solar Energy*, art. ID. 370823, **DOI:10.1155/2013/370823**.